

Automated Decision Support System for Tuberculosis Digital Images Using Evolutionary Learning Machines

E. Priya¹, S. Srinivasan¹

¹ Department of Instrumentation Engineering, Madras Institute of Technology, Anna University, Chennai

Abstract

Background: Tuberculosis (TB) is a major cause of illness and death in many countries, especially in Asia and Africa. Repeated tests of microscopic examination are needed to be performed for early detection of the disease. Hence there is a need to automate the diagnostic process for improvement in the sensitivity and accuracy of the test.

Objective: To automate the decision support system for tuberculosis digital images using histogram based statistical features and evolutionary based extreme learning machines.

Materials and methods: The sputum smear positive and negative images recorded under standard image acquisition protocol are subjected to histogram based feature extraction technique. Most significant features are selected using student 't' test.

These significant features are further used as input to the differential evolutionary extreme learning machine classifier.

Results: Results demonstrate that the histogram based significant features are able to differentiate TB positive and negative images with a higher specificity and accuracy.

Conclusion: The methodology used in this work seems to be useful for the automated analysis of TB sputum smear images in mass screening disorders such as pulmonary tuberculosis.

Keywords

Tuberculosis, sputum smear, histogram, differential evolution, extreme learning machines

Correspondence to:

S. Srinivasan

Department of Instrumentation Engineering,
Madras Institute of Technology
Address: Anna University, Chennai – 600 044
E-mail: srini@mitindia.edu

EJBI 2013; 9(2):3–8

received: January 9, 2013

accepted: March 25, 2013

published: August 30, 2013

1 Introduction

Tuberculosis (TB) is a communicable disease for which early diagnosis is critical to control the disease. Sputum smear microscopy continues to be the most widely used TB diagnostic method. The microscopy based TB screening method provides significant benefit to a large number of TB burdened communities across the globe [1].

The International Union Against Tuberculosis and Lung Disease recommend at least 100 view fields to be examined per sputum sample. The number of bacilli in these view fields is counted to grade the severity of the disease [2].

Manual screening using microscope is a conventional method employed for TB identification but it is tedious and requires highly trained experts [3]. Besides huge variability in sensitivity, manual screening for bacillus identification is a labor intensive task.

It consumes 40 minutes to 3 hours depending on patient's level of infection and it is needed to analyse 40 to

100 images of one slide. Hence automatic methods for TB identification are highly demanded [3, 4].

Several image analysis techniques have been reported for the automatic identification and classification of sputum smear samples [4, 5, 6]. Image histogram is an important digital image tool that represents the statistical information of the data within an image. The shape of the histogram provides many clues to the characteristics of the image. Different useful features from the histogram describe quantitatively the first and higher order statistical properties of the image. Common features include mean, variance, skewness, kurtosis, energy and entropy [7]. In order to classify the TB images into positive and negative, most significant features are derived from the original data sets. These significant features are used as input to the evolutionary based learning machine for the classification of sputum smear images into TB positive and negative.

Various machine learning techniques have been applied in classifying the TB positive and negative images.

The hybrid approach which takes advantages of both Differential Evolution (DE) and Extreme Learning Machine (ELM) has a more compact network. The DE process is a global searching optimization method used to tune the input weights and hidden layer biases where the output weights are determined by the generalized inverse procedure. The ELM learning algorithm is faster and has good generalization ability. The ELM algorithm overcomes many issues in traditional gradient algorithms such as stopping criterion, learning rate, number of epochs and local minima. On account of these advantages, DE-ELM has been effectively used in the field of medical diagnosis [8, 9].

In this work, histogram based statistical features are extracted from the sputum images. Most significant features are further given as input to the DE-ELM classifier to classify the TB positive and negative images.

2 Methods and Materials

2.1 Image Acquisition

The digital images of TB sputum smears captured using a fluorescence microscope at magnification $20\times$ with a camera in monochrome binning mode are used for this analysis. The digitized sputum smear images ($N = 100$) are subjected to histogram based feature extraction to identify and classify the images into TB positive and negative.

2.2 Histogram Based Statistical Features

The histograms are constructed by quantizing the image into bins. The statistical features such as mean, variance, skewness, kurtosis, energy and entropy are calculated by the probability distribution of intensity levels in the histogram bins. The statistical feature mean represents the brightness of the image. The mean measures the average value of intensity values. The image is bright if mean value is high and dark if it is low. The variance is the second order moment and it shows the contrast of gray level intensities. The low value of the variance indicates low contrast and the high value shows the high contrast of the image [10].

Skewness is a third order moment and it measures the inequality of intensity level distribution about the mean. The negative skewness value indicates a large number of intensity values on the right side of the mean or the tail on the left side is longer than the right side. The positive value indicates a large number of intensity values on the left side of the mean or the tail on right side is longer than the left side. The zero value indicates that the distribution of the intensity values is relatively equal on both sides of the mean [11].

The fourth order moment kurtosis is used to measure the peak distribution of intensity values around the mean. The high value of kurtosis indicates a sharp peak distri-

bution with long and fat tail. The low value of kurtosis indicates a rounded peak distribution with short and thin tail. The kurtosis of normal distribution is three. Kurtosis value is greater than three for the distributions that are more outlier prone than normal distribution. Distributions that are less outlier prone have kurtosis less than three [10].

The energy feature measures the uniformity of intensity level distribution. If the value is high, then the distribution is to a small number of intensity levels. The entropy measures the randomness of the distribution of the coefficients values over the intensity levels. If the value of entropy is high, then the distribution is among more intensity levels in the image and this measurement is the inverse of energy [10].

The mathematical formulations of the statistical features extracted from the histogram are given in Table 1. The n^{th} moment of the normalized gray level histogram is given by:

$$\mu_n = \sum_{l=1}^L (k_l - m)^n p(k_l) \quad (1)$$

where k_l is the gray value of the l^{th} pixel, m is the mean gray value of the pixel, L is the number of distinct gray levels, $p(k_l)$ is the normalized histogram representing the probability density function of the pixel [11, 12, 13].

Table 1: Mathematical formulations of histogram based statistical features.

Features	Formula
Mean	$m = \sum_{l=1}^L k_l p(k_l)$
Variance	$\sigma^2 = \sqrt{\sum_{l=1}^L (k_l - m)^2 p(k_l)}$
Skewness	$H_S = \frac{1}{\sigma^3} \sum_{l=1}^L (k_l - m)^3 p(k_l)$
Kurtosis	$H_K = \frac{1}{\sigma^4} \sum_{l=1}^L (k_l - m)^4 p(k_l) - 3$
Energy	$H_E = \sum_{l=1}^L \{p(k_l)\}^2$
Entropy	$H_N = - \sum_{l=1}^L p(k_l) \log\{p(k_l)\}$

To choose the most significant features, student 't' test is performed over the feature sets for further classification of the sputum smear images. The statistically significant ($p < 0.0001$) features chosen are mean, skewness and kurtosis.

2.3 Differential Evolutionary Extreme Learning Machines

Differential evolution proposed by Storn and Price is a global searching optimization method which obtains more compact network than the original ELM, as they require a large number of hidden units and long time for responding to new input patterns [9]. The network archi-

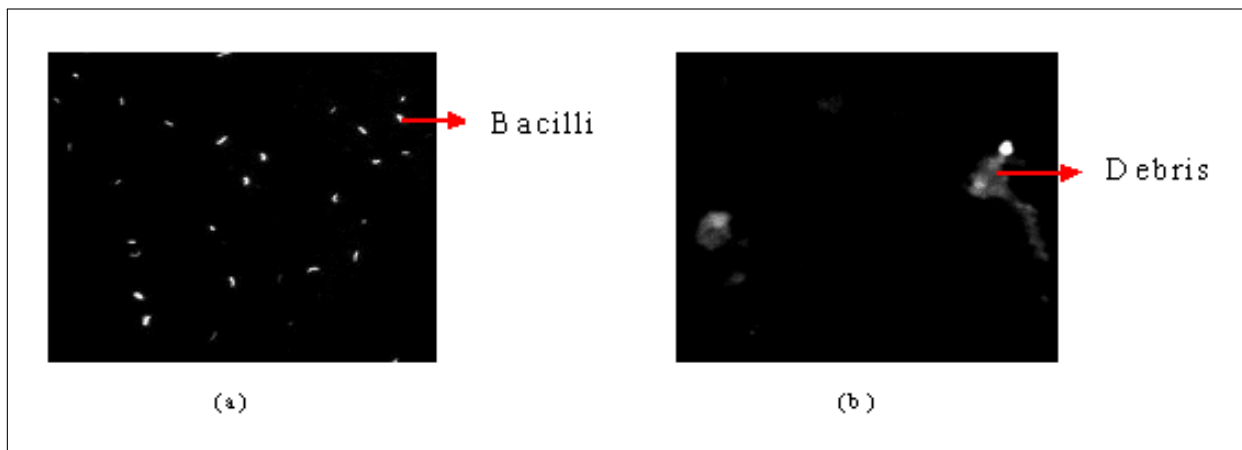


Figure 1: Typical TB (a) positive and (b) negative sputum smear image.

texture comprises of three layers such as input, hidden and output each consisting of one layer and is trained with K hidden neurons to learn N distinct samples. In the ELM algorithm, the network weights w_i and bias b_i are randomly assigned. The hidden layer output matrix, $H = \{h_{ij}\} (i = 1, \dots, N \text{ and } j = 1, \dots, K)$ is then calculated where $h_{ij} = g(w_j \cdot x_i + b_j)$ denotes the output of the j^{th} hidden neuron with respect to the input x_i and $g(x)$ represents the activation function. Finally, the output weight β is computed from the least square solutions $\beta = H^\dagger T$, where H^\dagger is the Moore-Penrose generalized inverse of H and $T = [t_1, \dots, t_N]^T$ is the matrix of desired outputs [8]. The Root Mean Square Error (RMSE) between the test target and the actual target is calculated. The RMSE of testing samples is used as a standard to analyze the testing accuracy, which is affected by the number of hidden neurons and activation function. Classification accuracy increases with decrease in RMSE and reflects the discrepancy between the actual and target values and is evaluated as [14]

$$RMSE = \sqrt{\frac{\sum_{i=1}^N \|\sum_{j=1}^K \beta_j g(w_j x_i + b_j) - t_i\|_2^2}{N}} \quad (2)$$

The performance of the classifier is tested using sensitivity, specificity and accuracy. Sensitivity is referred to the fraction of positive images correctly classified as positive, specificity is referred to the fraction of negative images correctly classified as negative and accuracy is referred to the ratio of correctly classified images to the total images.

3 Results and Discussion

Typical representative of TB positive and negative smear images are shown in Figures 1 (a) and (b) respectively. TB positive image shows the presence of rod shaped bacilli objects on a dark background. The negative images may contain scanty or absence of bacilli. The spu-

tum smear images considered contain debris, which can be due to poor or nonspecific staining of the smear slides and due to overlapping bacilli. These debris objects do not have uniform morphology. Histogram based statistical features are extracted from these images to extract useful statistical information that aid in differentiating the images into TB positive and negative.

The normalized average and standard deviation values of the histogram based statistical features for TB positive and negative images are shown in Table 2. It is observed that the average values of the features mean, variance, skewness, kurtosis and entropy except energy are found to be high for TB positive images than negative. The mean intensity value of positive images is higher than the negative that represents the brightness of the image. Since the number of bacilli in TB negative images is lower, the brightness is less and image is dark as represented by the mean feature in Table 2.

Table 2: Average and standard deviation values of the histogram based statistical features.

Histogram based statistical features	Average \pm SD	
	TB positive	TB negative
Mean	0.87 \pm 0.03	0.83 \pm 0.02 *
Variance	0.27 \pm 0.19	0.16 \pm 0.16
Skewness	0.56 \pm 0.17	0.30 \pm 0.18 *
Kurtosis	0.32 \pm 0.18	0.11 \pm 0.15 *
Energy	0.97 \pm 0.05	0.97 \pm 0.03
Entropy	0.29 \pm 0.24	0.17 \pm 0.10

* ($p < 0.0001$) highly statistically significant

TB positive images consists of a large number of rod shaped objects, hence the contrast is comparatively higher than negative images. Contrast of TB negative images is lower because of the absence or presence of scanty number of bacilli exhibiting a lower variance value. The positive skewness of both positive and negative indicates the uniformity of background intensity values. Because of the

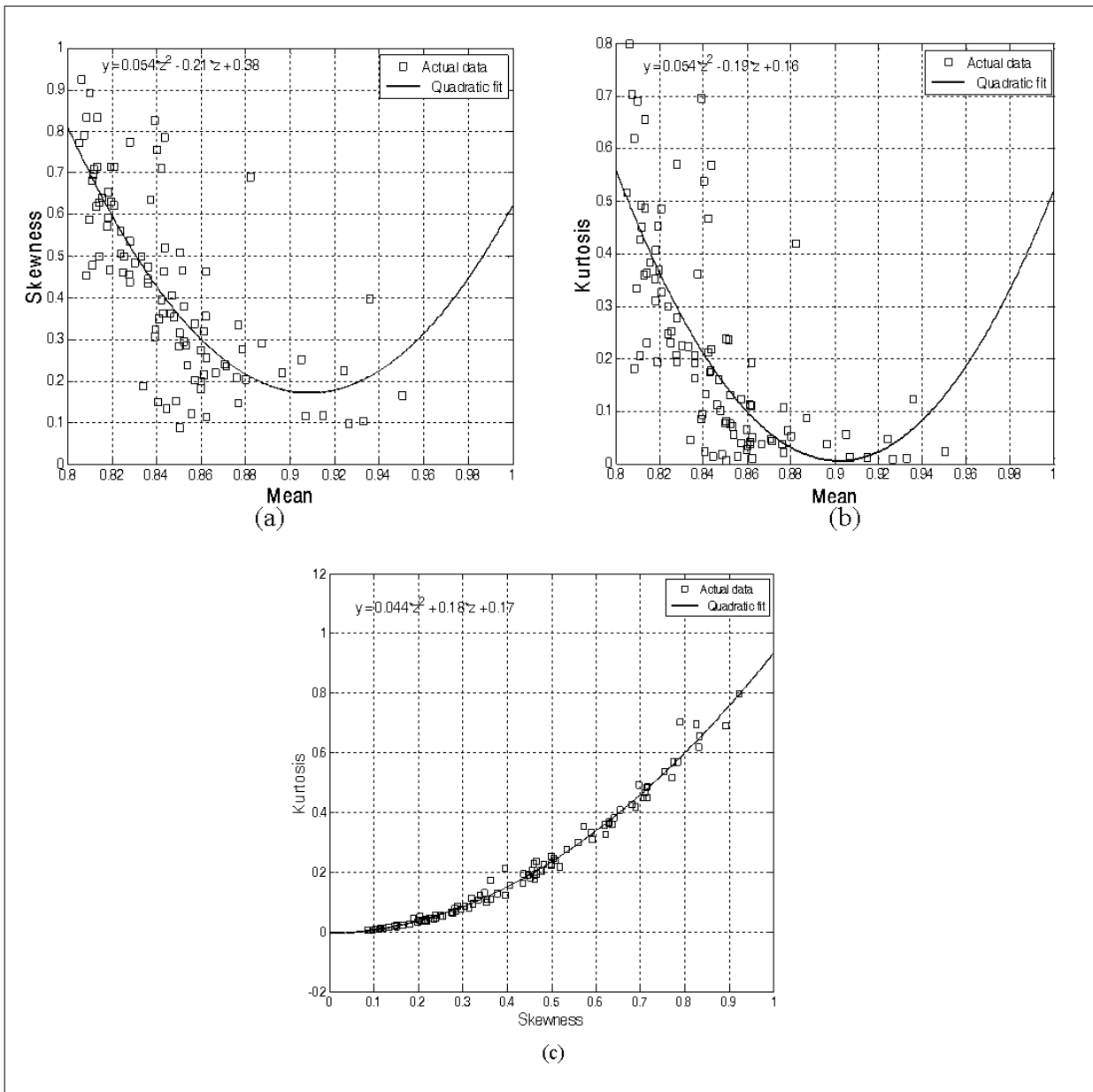


Figure 2: Quadratic fit of (a) skewness (b) kurtosis as a function of mean values (c) kurtosis as a function of skewness value.

presence of numerous foreground objects (bacilli) in positive images, the skewness is higher than negative.

The higher value of kurtosis is due to the sharp change in gray level that arises around the edge of bacilli and smears in the positive images. The energy feature measures an equal value which measures the uniformity of intensity level distribution in both positive and negative images. The entropy is observed to be high for positive images as the distribution is among more intensity levels than negative. To reduce the complexity in classifying the positive and negative images the most significant features are chosen using student 't' test. Table 2 shows the highly statistically significant ($p < 0.0001$) features mean, skewness and kurtosis.

Quadratic fit of skewness and kurtosis as a function of mean values are shown in Figures 2 (a) and (b). The mean

value of TB positive images is 0.87 that differs from that of negative which is about 0.83. The plot in Figure 2 (a) shows the variation of average intensity with respect to the distribution of intensity values for both positive and negative images. It is observed that the two (TB positive and negative) groups centred on the mean value assist in classification of these images. Similarly Figure 2 (b) shows the variation of average intensity with respect to degree of peaked-ness of the distribution.

The quadratic fit of kurtosis as a function of skewness value is shown in Figure 2 (c). It is observed that the skewness value of TB positive images is centered on 0.56 and for negative images it is centered on 0.30. Also, Figure 2 (c) presents the variation in distribution of intensity values with respect to degree of peaked-ness. In order to differentiate the positive and negative images, the

three significant features are further given as input to the DE-ELM classifier.

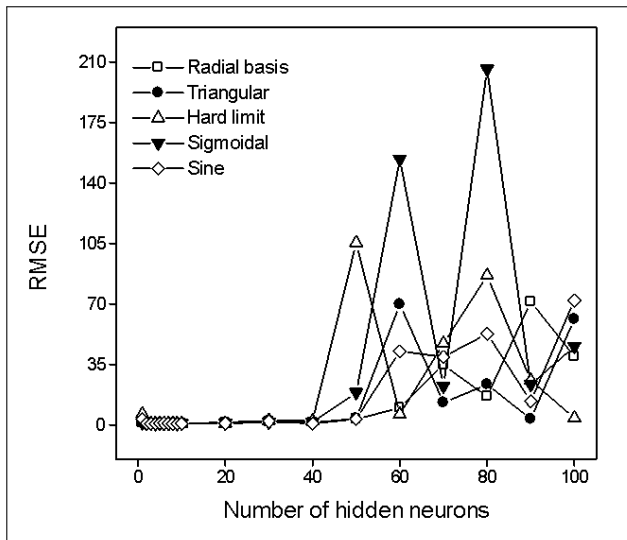


Figure 3: Error plot for varying number of hidden neurons and activation function.

The performance of the classifier is evaluated using RMSE by varying the number of hidden neurons as shown in Figure 3. The evaluation is performed for different activation function such as radial basis, triangular, hard limit,

sigmoidal and sine. The corresponding RMSE values are presented in Table 3.

It is observed from Table 3 that radial basis activation function seems to perform with a lower RMSE value (0.637) for ten numbers of hidden neurons. Hence radial basis activation function is considered for further analysis of the classifier.

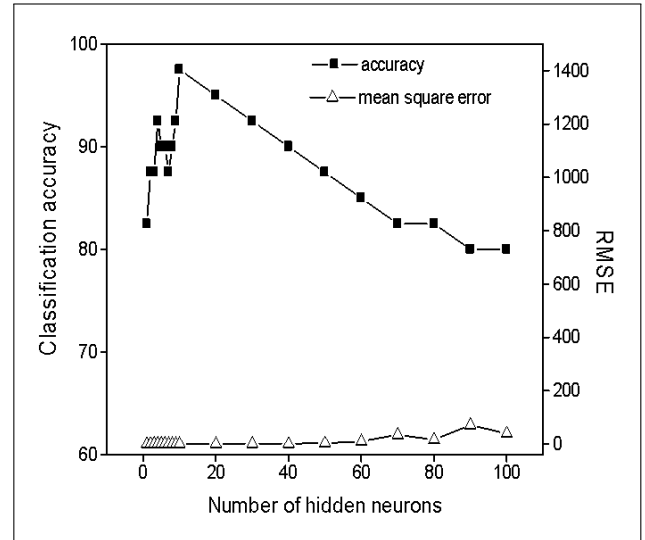


Figure 4: Error plot for varying number of hidden neurons and activation function.

Table 3: RMSE for varying number of hidden neurons and activation function.

No. of hidden neurons	RMSE for different activation function				
	Radial basis	Triangular	Hard limit	Sigmoidal	Sine
1	1.055	3.073	6.252	0.957	3.243
2	0.747	0.816	0.837	0.810	0.771
3	0.806	0.802	0.732	0.785	0.770
4	0.838	0.757	0.717	0.724	0.655
5	0.927	0.750	0.762	0.893	0.723
6	0.715	0.779	0.755	0.833	0.834
7	0.723	0.711	0.732	0.718	0.735
8	0.686	0.675	0.729	0.716	0.706
9	0.651	0.652	0.717	0.694	0.683
10	0.637	0.753	0.687	0.851	0.713
20	1.225	1.368	0.718	0.922	0.881
30	1.831	2.397	2.418	1.479	2.069
40	1.427	0.827	2.305	1.506	0.733
50	3.186	3.637	105.334	18.671	3.297
60	9.800	69.665	6.010	153.675	42.551
70	34.667	12.810	47.046	22.404	39.253
80	16.367	23.439	86.396	205.710	52.618
90	71.383	3.315	25.680	23.258	13.691
100	39.535	61.134	3.892	45.384	71.945

* ($p < 0.0001$) highly statistically significant

The error plot and classification accuracy is shown in Figure 4 for different number of hidden neurons with radial basis function as the activation function. The number of hidden neurons is observed to be ten for the minimum RMSE and maximum classification accuracy.

Table 4: Confusion matrix of the classifier.

Confusion matrix		Predicted class	
		Positive (train/test)	Negative (train/test)
Actual class	Positive (train/test)	28/17	02/03
	Negative (train/test)	00/00	30/20

Table 4 shows the confusion matrix of the classifier, presenting the actual and the predicted classes for both training and testing. Since all the negative images subjected to this methodology are predicted correctly, specificity of both training and testing is observed to be 100%. Except three of the 40% test data remaining are correctly predicted and thus the accuracy is observed to be 92.5% with a training accuracy of 96.7%.

4 Conclusion

Any person with active tuberculosis is capable of infecting on average between 10 and 15 people every year [15]. Therefore, early automated detection of the disease is vital for monitoring, control and for treatment of tuberculosis.

In this work, an attempt has been made to automate the decision support system for tuberculosis digital images using histogram based statistical features and evolutionary based extreme learning machines. Results demonstrate that the significant histogram features are able to differentiate TB positive and negative images with a higher specificity and accuracy. Thus the methodology seems to be useful for the automated analysis of TB sputum smear images in mass screening disorders such as pulmonary tuberculosis.

Acknowledgements

The authors acknowledge Tania S. Douglas of Medical Imaging Research Unit, University of Cape Town, South Africa for the sputum smear images.

References

- [1] Chang J., Arbelaez P., Switz N., Reber C., Tapley A., Davis L., Cattamanchi A., Fletcher D., Malik J. Automated tuberculosis diagnosis using fluorescence images from a mobile microscope. Ayache N. et al. Editors. MICCAI 2012, Part III, LNCS, 2012; 7512: 345-352.
- [2] Laszlo A. Technical Guide, Sputum examination for tuberculosis by direct microscopy in low income countries, Fifth edition 2000, International Union Against Tuberculosis and Lung Disease, Paris, France.
- [3] Zhai Y., Liu Y., Zhou D., Liu S. Automatic identification of mycobacterium tuberculosis from ZN-stained sputum smear: Algorithm and system design, in Proceedings of the IEEE International Conference on Robotics and Biomimetics, 2010, Tianjin, China, 41-46.
- [4] Sotaquira M., Rueda L., Narvaez R. Detection and quantification of bacilli and clusters present in sputum smear samples: a novel algorithm for pulmonary tuberculosis diagnosis, in Proceedings of the International Conference on Digital Image Processing, 2009, Bangkok, Thailand, 117-121.
- [5] Khutlang R., Krishnan S., Whitelaw A., Douglas T.S. Automated detection of tuberculosis in Ziehl-Neelsen-stained sputum smears using two one-class classifiers. J Microsc. 2010; 237: 96-102.
- [6] Forero M.G., Cristobal G., Desco M. Automatic identification of mycobacterium tuberculosis by Gaussian mixture models. J Microsc. 2006; 223:120-132.
- [7] Srinivasan G.N., Shobha G. Statistical Texture Analysis, in Proceedings of World Academy of Science, Engineering and Technology, 2008; 36: 1264-1269.
- [8] Huynh H.T., Won Y. Hematocrit estimation from compact single hidden layer feedforward neural networks trained by evolutionary algorithm, IEEE Congress on Evolutionary Computation, 2008, Hong Kong, 2962-2966.
- [9] Yusoff I.A., Isa N.A.M., Othman N.H., Sulaiman S.N., Jusman Y. Performance of neural network architectures: Cascaded MLP versus extreme learning machine on cervical cell image classification. In Proceedings of 10th International Conference on Information Science, Signal Processing and their Applications, 2010, Kuala Lumpur, Malaysia, 308-311.
- [10] Seetha M., Malini Devi G., Sunitha K.V.N. Performance assessment of feature based image retrieval using neural networks, International Journal of Systems, Algorithms Applications, 2012, 2: 4-8.
- [11] Shi X., Cheng H.D., Hu L. Mass detection and classification in breast ultrasound images using fuzzy SVM, in Proceedings of the Joint Conference on Information Science, 2006.
- [12] Nurhayati O.D., Widodo T.S., Susanto A. Tjokronagoro M. First order statistical feature for breast cancer detection using thermal images, World Academy of Science, Engineering and Technology, 2010, 46: 424-426.
- [13] Younus A.M., Widodo A., Yang B.S. Evaluation of thermography image data for machine fault diagnosis, Nondestr Test Eval. 2010; 25: 231-247.
- [14] Zhu Q.Y., Qin A.K., Suganthan P.N., Huang G.B., Evolutionary extreme learning machine, Pattern Recognit. 2005, 38: 1759-1763.
- [15] Tuberculosis Fact. World Health Organization (WHO), Geneva, 2010, Sheet No. 104.